

Molecular BioSystems

Accepted Manuscript



This is an *Accepted Manuscript*, which has been through the Royal Society of Chemistry peer review process and has been accepted for publication.

Accepted Manuscripts are published online shortly after acceptance, before technical editing, formatting and proof reading. Using this free service, authors can make their results available to the community, in citable form, before we publish the edited article. We will replace this *Accepted Manuscript* with the edited and formatted *Advance Article* as soon as it is available.

You can find more information about *Accepted Manuscripts* in the [Information for Authors](#).

Please note that technical editing may introduce minor changes to the text and/or graphics, which may alter content. The journal's standard [Terms & Conditions](#) and the [Ethical guidelines](#) still apply. In no event shall the Royal Society of Chemistry be held responsible for any errors or omissions in this *Accepted Manuscript* or any consequences arising from the use of any information it contains.



www.rsc.org/molecularbiosystems



Journal Name

ARTICLE

Amphotericin B and Anidulafungin Directly Interact with DNA and Induce Oxidative Damage in Mammalian Genome

Received 00th January 20xx,
Accepted 00th January 20xx

DOI: 10.1039/x0xx00000x

www.rsc.org/

Santi M Mandal^{a,b,*}, Anirban Chakraborty^b, Maidul Hossain^c, Denial Mahata^a, William F. Porto^d, Ranadhir Chakraborty^e, Chinmay K. Mukhopadhyay^f, Octavio L. Franco^d, Tapas K. Hazra^b, Amit Basak^a

Amphotericin B and anidulafungin are widely used antifungal drugs for the treatment of systemic and serious mycoses. Amphotericin B is relatively toxic drug, has long been established. This study is first of its kind to systematically investigate the nature of binding to DNA, and to evaluate intercalation of AMP-B or ANIDULA with the aid of UV-Vis, ITC, and CD spectroscopy. The binding affinity of AMP-B with exclusion sites of 4.68 base pairs ($1.2 \times 10^5 \text{M}^{-1}$) was found to be higher than ANIDULA with exclusion sites of 6.67 base pairs ($3.78 \times 10^4 \text{M}^{-1}$); consistent with the binding affinity values obtained for AMP-B (10^5M^{-1}) and ANIDULA (10^4M^{-1}). The binding of two drugs with double-stranded DNA was favoured by negative enthalpy as well as negative entropy changes. The intercalation of drugs to duplex polynucleotide induced changes in the intrinsic CD spectra revealed comparatively higher affinity towards AMP-B than ANIDULA. Molecular docking studies revealed that the negative binding energy was higher in case of AMP-B reflecting more affinity towards single-stranded DNA. The results of the cytotoxicity, immunoblotting, and gene specific LA-QPCR assay have indicated that ANIDULA is less genotoxic than AMP-B. Hence, the superiority of ANIDULA over AMP-B as systemic antifungal drug has been established beyond doubt.

Introduction

Incidence of systemic fungal infections has increased from the last quarter of the preceding century because of rampant use of broad-spectrum antibiotics, extensive cytotoxic chemotherapy, higher frequency of stem cell therapy along with organ transplantation, and the execution of prosthetic devices and use of indwelling intravascular catheters. Among all fungal pathogens that create medical problem, *Candida* tops the list in causing systemic infections and sometimes are

life-threatening in immuno-compromised patients. For many years, before the advent of echinocandins and the clearance of its recent-most derivative, anidulafungin, as drug after clinical trials, the cytosine analogue (5-fluorocytosine), triazole compounds (particularly fluconazole), and polyenes (more specifically amphotericin B) have been used most extensively in treating fungal infections¹. Emergence of resistance of the fungal pathogens towards azoles and 5-fluorocytosine²⁻⁴ has in turn led the clinicians to opt for the only choice, polyene-based compounds (in spite of their toxicity), particularly amphotericin-B in the treatment of resistant-*Candida* infections. Hence, discovery of echinocandins was a welcome development in antifungal therapy. Echinocandins inhibit cell wall biosynthesis in fungi by interrupting the synthesis of 1,3-beta-D-glucan¹. Since mechanism of action of echinocandins differed from the mode of action(s) of azoles (inhibits sterol biosynthesis), polyenes (directly interacts with cell membrane sterols), and fluocytosine (interferes with the nucleic acid metabolism), rapid appearance of resistance to anidulafungin is not very probable. Resistance to anidulafungin in isolates can occur only if mutations are

^aCentral Research Facility, Department of Chemistry, Indian Institute of Technology Kharagpur Kharagpur 721302, India. ^bDepartment of Internal Medicine, University of Texas Medical Branch, Galveston; TX 77555, USA. ^cDepartment of Chemistry, Vidyasagar University, Midnapore 721102, WB, India. ^dDepartment of Biology, Institute of Biological Sciences, Graduate Program in Genetics and Biotechnology, Federal University of Juiz de Fora, Juiz de Fora-MG, 36036-900, Brazil. ^eDepartment of Biotechnology, North Bengal University, Siliguri- 734013, Darjeeling, India. ^fSpecial Centre for Molecular Medicine, Jawaharlal Nehru University, New Delhi 110 067, India. ^gPresent Address: Anti-Infective Research Lab, Department of Microbiology, Vidyasagar University, Midnapore 721102, WB, India.

*Author to whom correspondence should be addressed: E.mail: mandalsm@gmail.com Telephone: +91-3222-282486, Fax: 91-3222-282481,

† Footnotes relating to the title and/or authors should appear here. Electronic Supplementary Information (ESI) available: [Cytotoxicity analysis of antifungal drugs and analysis of genotoxic effect in terms of DNA strand break accumulation. See DOI: 10.1039/x0xx00000x]

recruited in the genes that expresses 1,3-beta-D-glucan synthase enzyme complex. Amphotericin B is a cyclic amphiphilic molecules (Fig. 1) binding to the ergosterol and lipid bilayer, make pores in the membrane facilitate the leakage of small cations like K^+ , Na^+ , and Ca^{2+} (7). Anidulafungin is noncompetitive inhibitors of β -D-glucan synthase, an enzyme helps to synthesize (1 \rightarrow 3)- β -D-glucan cell wall component¹. Again, abundance of beta-1,3-bonds in the fungal cells will render the pathogen susceptible to anidulafungin *in-vitro* for sure. Other positive points in favor of anidulafungin therapy are: (i) it does not induce, inhibit, or get used as substrate of the cytochrome P450 enzyme system ruling out any major drug interaction; (ii) the ring-form of anidulafungin is non-enzymatically degraded to linear peptide followed by further degradation to simpler forms with the aid of non-specific peptidases present in the human plasma (binding to human plasma protein is 99%); (iii) it is eliminated through fecal route and do not pose environmental risk as it is readily degraded; (iv) it is found not to be 'genotoxic' at least from the test results of bacterial reverse mutation assays (Ames test), *in-vitro* chromosome aberration tests in CHO cell line or mouse lymphoma cells, and *in-vivo* mouse micronucleus test. Summing up all the points, FDA approved the use of anidulafungin for the treatment of invasive candidiasis, candidemia and esophageal candidiasis.

What really absent was the carcinogenicity test of anidulafungin. Long-term carcinogenicity studies with anidulafungin were not conducted nor anticipated because it showed no selective reproductive or developmental toxicity or genotoxicity *in-vitro* envisaged in the tests as mentioned earlier. Besides all advantages, it is poorly bio-available (5%) and the only route for administration is intravenous. Studies in murine samples demonstrated persistence of intravenously administered anidulafungin (single dose) in tissues for many days⁵. Anidulafungin's retention in the tissue for days poses a potential biological question of inflicting DNA damage, if any. In the present study, we have performed a detail study to test the ability of anidulafungin to cause DNA damage with reference to the activity shown by another most widely used systemic antifungal compound, amphotericin B, under the same dosage and reaction conditions. The study has been successful to confer the superiority of anidulafungin over amphotericin B in terms of lesser DNA damage activity; and the results of our experiments stand as a gap-filler to rule out the potentiality of being a carcinogen.

Results and discussion

Absorption spectroscopy and binding affinity evaluation

Interaction of small molecules with DNA can be suitably monitored using electronic spectroscopy by the changes in the absorbance and the shift in the wavelength maxima. The effect of progressively increasing the concentration of DNA on the absorption spectrum of AMP-B and ANIDULA are presented in Fig. 2. The characteristic hypochromism, sharp isosbestic points and saturation at high DNA concentrations suggest a simple two state transition between the free and bound drug. The absorbance spectrum of AMP-B in solution shows absorption maxima at 407, 384, 363 and 323 nm with a sharp isosbestic points at 298nm. On the other hand anidula shows maxima at 288 nm and isobastic points at 291 nm. Since no evidence for any cooperatively (no positive slope at low input values of the drug) was found, the Scatchard plots were analyzed by the McGhee-von Hippel equation⁸ for non-cooperative ligand binding. The solid lines represent the best fit of the experimental value to equation (1). The result obtained from the experiment is that the entire DNA binding to these drugs occurred non-cooperatively. The binding affinity (k) of amp-B with DNA was $1.20 \times 10^5 M^{-1}$ with exclusion sites (n) of 4.68 base pairs. On the other hand, the binding affinity (k) value for anidula was $3.78 \times 10^4 M^{-1}$ with exclusion sites (n) of 6.67 base pairs.

Isothermal titration calorimetry

Binding of small molecules to macromolecules can be conveniently monitored by using isothermal titration calorimetry (ITC)^{6,18}. The benefit of ITC is that it can give complete thermodynamic profile of the binding, for instance, Gibbs free energy (ΔG), enthalpy change (ΔH), and entropy change together with an estimate of the binding affinity (K) and the stoichiometry (n) in a single-shot experiment. The representative ITC profiles of the binding of AMP-B and ANIDULA to dsDNA were presented in Figure 3. Upper panels showed the representative raw ITC profiles resulting from the titration of amp-B and Anidula binding to the DNA under study. The data from ITC experiments are presented in Table 1. It can be seen that the binding affinity values obtained from ITC data are of the order of $10^5 M^{-1}$ order for AMP-B with double stranded DNA and $10^4 M^{-1}$ order for ANIDULA which is very much consistent with value obtained from the absorption titration studies. The binding of these drugs

with dsDNA was favored by negative enthalpy as well as negative entropy changes but the value of negative enthalpy was much higher for anidula. The free energy change in each case was more or less similar (around 6.45–6.85 kcal mol⁻¹). To understand the base pair specificity of these two drugs towards DNA bases, four sequences of DNA namely AG, AT, GC and TC was incorporated in this study. The binding constant obtained from these experiments revealed that Amp-B has highest binding affinity for GC and the degree of binding followed the order GC>TC>AG>AT. The binding of Amp-B to GC and TC was favored by strong negative enthalpy and entropy while with AG was favored by small negative enthalpy and positive entropy. The energetic of the binding with AT DNA was totally different from these three types of DNA sequences. The positive enthalpy and positive entropy change indicate an enthalpically unfavorable interaction. The positive sign of both the enthalpy and entropy term can be considered as a characteristic of a predominantly hydrophobic binding reaction [6]. On the other hand anidula shows highest binding towards AG and varying in the order AG>TC. The binding of anidula to AG was favored by negative enthalpy and entropy where as the binding of TC was fully dependant on the unfavourable enthalpy and favorable entropy change. In AT and GC, the thermogram revealed unusual binding that could not be fitted to any protocol. The values obtained from these experiments were similar to that observed for other intercalators⁶.

CD analysis

Circular dichroism is an instructive technique that can give information about the binding mode. The intercalation of AMP-B and ANIDULA to duplex polynucleotides induced changes in the intrinsic CD of the polynucleotides. Comparative circular dichroic changes in the polynucleotides on binding of AMP-B and ANIDULA at various D/P (drug/ polynucleotide base pair molar ratio) values were recorded in the 180–300 nm regions. The data are presented in Figure 4. The binding results in terms of the enhancement in the ellipticity of the long wavelength positive (266 nm) and negative(250 nm) bands reflected lengthening of the helix and weakening of the base stacking interactions due to intercalation; and the change was more prominent in case of AMP-B compared to that of anidula. This result clearly indicated that the nucleotide-binding-affinity of AMP-B was much higher and therefore it is in good agreement with the UV and ITC value.

Molecular docking

AMP-B and ANIDULA were docked against SS DNAs composed of AG, AT, CG and CT. Overall, AMP-B showed a more negative binding energy than ANIDULA, reflecting in more affinity to SS DNA (Fig. 5), which is in agreement with ITC and CD analysis. However, analyzing each complex separately, only the complexes of AG and AT with AMP-B could represent the real binding mode, as they demonstrated binding energies virtually identical to ITC results.

Cytotoxicity/Immunoblotting/ oxidative DNA damage

In order to evaluate the cytotoxicity level of antifungal drugs, MTT assay was performed with different doses of the drugs. Results revealed that amphotericin B is more toxic than anidulafungin in same concentration (Fig. S1). To account for the genotoxic effect of the antifungal drugs, the expression level of a number of DNA repair proteins (NEIL1, NEIL2, OGG1, Nth1, APE1 and PNKP) were monitored in whole cell extract in response to the treatment with different doses of the antifungal agents (Fig. 6). The levels of the repair proteins were found to be enhanced after treatment with both the antifungal agents, individually. The expression of repair proteins followed a consistent pattern in both the cases. Among them, however, increase in the level of NEIL2, APE1 and PNKP stood out to be significant in comparison to the other proteins and fold enhancement was more prominent for the Amphotericin B treatment as compared to treatment by Anidulafungin with respect to NEIL2 and PNKP expression. NEIL2 is an oxidized base specific human DNA glycosylase which uniquely excise oxidized bases from base-unpaired sequences in DNA. The protein, APE1 cleaves the phosphodiester backbone immediately 5' to an AP site, via hydrolytic mechanism, to generate a single-strand DNA break leaving a 3'-hydroxyl and 5'-deoxyribose phosphate terminus. PNKP is one of the major DNA end processing enzyme with 3' phosphatase and 5' kinase activities and it generates 5'- phosphates and 3'-hydroxyl groups at the damaged DNA termini that are required for subsequent processing by DNA ligases and polymerases. The increase in the level of these proteins in response to drug treatment is indicative of the cytotoxic DNA damage effect that the antifungal agents may possess. To examine the accumulation of oxidized purine and pyrimidine base adducts and subsequent DNA strand breaks (DNA SB) before and after treatment, genomic DNA was isolated from HEK-293 cells treated with different doses of antifungal agents, and the levels of SBs in the HPRT and POLB gene was compared using long amplicon quantitative PCR (LA-

QPCR) as described previously^{16,17}. A decreased level of the long amplicon PCR product (~10-12 kb) would reflect a higher level of DNA SBs, and amplification of a smaller fragment for the gene should be similar for the samples, because of a lower probability of SB formation in a shorter fragment. We have indeed observed a higher level of DNA lesion frequency in the genomic DNA particularly with higher dose of the drug treatment compared to control cells (Fig. 7). The effect was more prominent for amphotericin B for both the genes as is evident in the Fig. S2. DNA strand breaks (SBs), both single-stranded (SSBs) and double-stranded (DSBs), are among the most toxic and mutagenic lesions in mammalian genomes. Among them, various “dirty” DNA ends are extremely toxic because such ends block the action of DNA polymerases and DNA ligases; the conventional 3'-OH (hydroxyl) and 5'-P (phosphate) ends must be restored for gap-filling and DNA ligation to occur during repair for maintaining genomic integrity. Unrepaired SBs can have impact on the fate of the cell in several ways. The most likely effect in proliferating cells is the blockage or collapse of DNA replication forks during the S phase. Hence, SBs pose a significant threat to maintaining genomic integrity and cell survival. Our results show a sharp increase in the level of PNKP and the level of NEIL2 after treatment with the antifungal drugs. This is indicative of accumulation of DNA SBs as side effect of the treatment. Among them, human polynucleotide kinase 3'-phosphatase (PNKP) is a major DNA end-processing enzyme which removes the 3'-P group¹⁹ and catalyzes the phosphorylation of 5'-OH termini (generated by some nucleases, and as intermediates of topoisomerase cleavage; thus involved in the repair of both SSBs via the SSB repair (SSBR) pathway and DSBs via non-homologous end joining. Also, NEIL2 is an important mediator of base excision repair (BER) of oxidative DNA damage particularly for transcribing genes²⁰.

Materials and methods

UV-Vis spectroscopy

A Shimadzu Pharmaspec (Shimadzu Corporation, Kyoto, Japan) was used for absorption spectral studies. For this purpose a constant concentration of the DNA was treated with increasing concentration of the AMP-B/ANIDULA in one cm path length matched quartz cells with continuous stirring. The amount of free and bound drug was determined as described previously⁶⁻⁷. Binding data obtained from spectrophotometric titration of increasing concentrations of drug to a fixed concentration of DNA was

transmitted into the form of Scatchard plot of r/C_f versus r , where r is the number of ligand (drug) molecules bound per mole of DNA base pairs. Non-linear binding isotherms observed were fitted to a theoretical curve drawn according to the excluded site model of McGhee and von Hippel⁸ for non-cooperative ligand binding system using the following equation

$$r/C_f = K (1-nr)/\{1-(n-1)r\}^{(n-1)} \dots\dots\dots(1)$$

where K is the intrinsic binding constant to an isolated binding site, and n is the number of nucleotides occluded by the binding of a single ligand molecule.

Synthesis of Base Pairs

To understand the base pair specificity of these two drugs towards DNA bases, four oligo sequences of DNA namely AG, AT, GC and TC specific repeated sequences are synthesized as 5'-AGAGAGAGAGAGAGAG-3'; 5'-ATATATATATATATAT - 3'; 5'-GCGCGCGCGCGCGC-3' and 5'-TCTCTCTCTCTCTC-3' and used in further study.

Isothermal Titration Calorimetry (ITC)

The titration was performed using a ITC200 Systems (GE Healthcare, USA) coupled with non-reactive Hastelloy® cells for chemical resistance. The titrations were carried out 0.25 × 10⁻³ molar solution of DNA against 0.1 × 10⁻³ molar solution of each drug in PBS (1X) buffer. All solutions were degassed right before the experimental runs under same reaction condition at 25 °C and at 180 sec intervals utilizing a stir speed of 310 rpm. Blank ITC experiments were done to correct heat of dilution effects. Origin 7.0 (OriginLab Corp., MA) was used to analyze the ITC data to determine the binding constant (K) and enthalpy of binding (ΔH) directly from the binding thermograms.

Circular Dichroism Spectroscopy

The Circular dichroism (CD) spectrum was recorded at room temperature using a Jasco J-815 spectropolarimeter equipped with a Jasco PTC-423 S Peltier temperature controller. The scanning rate was 50 nm.min⁻¹ with a response time of 2s. Spectrum was recorded at standard sensitivity (100 mdeg) with a data-pitch of 0.5 nm continuous mode. The scanning range was 300-190 nm and the resultant spectrum was the average of two consequent accumulations. The baseline was corrected by subtracting the corresponding buffer blank.

Molecular Docking

The 2D structures of AMP-B and ANIDULA were obtained from KEGG database (IDs D00203 and D03211, respectively). The 2D structures were optimized for 3D structures through the PRODRG Server⁹. The Single Strand DNA (SS DNA) structures were obtained from the following pdb structures 1D56 for AT¹⁰, 1I0T for CG¹¹ and 196D for AG and CT¹². The docking was performed through AutoDock Vina¹³, where the DNA structures were used as receptors and the antibiotic structures were used as ligands. The structures were processed by AutoDock Tools¹⁴ and the grid box of 30 Å³ was set to the center of receptor. Each docking was repeated 50 times.

Cytotoxicity assay

MTT assay was performed to determine cell cytotoxicity following the method described earlier by Mandal et al.¹⁵. Human Embryonic kidney (HEK-293) cells (2.0×10^3) cells were seeded in 100 µL complete DMEM medium per well in 96 well plates. Plates were incubated at 37°C in 5% CO₂ for 24 hours for cell attachment. Cells were treated with individual compounds with variable concentration from 5-100 µg/mL and incubated at 37°C in 5% CO₂ for 48h. Three wells were used in the 96 well plates for each derivative and repeated three times. For the MTT assay, thiazolyl blue tetrazolium bromide solution (100µL; 1 mg/ mL) was added and the mixture was incubated for 4 hours. After that, 100 µL of dimethylsulphoxide (DMSO) was added and the plates were rotated for 5 minutes. Optical density was recorded at 550 nm with DMSO as blank. Percent cell viability was plotted against concentrations of derivatives. Cells treated without any compound were used as control.

Immunoblotting

Human Embryonic kidney (HEK-293) cells were treated with ANIDULA (Pfizer pharmaceutical) and AMP-B (X gen pharmaceutical) at final concentration of 5 µg/ml, 10 µg/ml, 20 µg/ml, 50 µg/ml and 100 µg/ml for 24 hours in 30 mm plates along with mock (without treatment). From a part of the cells, whole cell extract was prepared using RIPA buffer (Sigma) and 15 µg proteins (after quantitation by Bradford assay) was loaded in 4-12% Bis Tris gel (Invitrogen). After electrophoretic transfer of proteins to nitrocellulose membrane, the membranes were probed with following antibodies to check for the expression profile of the proteins before and after treatments: NEIL1, NEIL2, OGG1, NTH1, APE1 and PNKP (all were anti rabbit antibodies raised in laboratory conditions and antibody dilution was 1:500 in each

case). The human anti rabbit Lamin B antibody (Genetex Inc.) was used for checking equal loading of proteins in each lane. In each case, the blot was stripped using Restore Plus stripping buffer (Thermo scientific) and reprobed with another antibody. Finally, the band intensities were quantified using ImageJ software and normalized with band intensities of the loading control.

Gene-specific LA-QPCR assays

Another part of the above treated cells were harvested for genomic DNA extraction using the QIAGEN Genomic-tip 20/G kit (Qiagen) as per the manufacturer's directions. This kit is particularly useful, as it minimizes DNA oxidation during the isolation step and has been previously used for LA-QPCR assays¹⁷. After quantitation by Pico Green (Molecular Probes) in a 96-well black bottomed plate, the genomic DNA was digested with the *E. coli* enzymes Fpg (NEB) and Nei (NEB), which are able to remove a variety of oxidized purine and pyrimidine bases and to induce strand breaks at the sites of unrepaired oxidized base by cleaving the phosphodiester bond with their associated AP lyase activity, facilitating efficient detection of DNA damage by inhibiting *Taq* polymerase to surpass the lesion site, thereby decreasing the amplification efficiency. *E. coli* enzymes are chosen for the purpose of inducing strand breaks because of their robust activity to remove oxidized bases on double stranded DNA whereas Nei homologs in mammalian cells, like NEIL2 prefers lesions in single-stranded DNA over duplex DNA and interacts with a number of transcription factors, *in-vivo*, including RNA polymerase II, which help to open up the DNA strands and thus, to remove bases in a transcription-coupled repair pathway²⁰. Gene-specific LA-QPCR assays¹⁶⁻¹⁷ for measuring DNA damage were performed using Long Amp *Taq* DNA Polymerase (New England Biolabs) to amplify a 10.4 kb region of the HPRT or 12.2 kb of the POLB gene in human genomic DNA using the following primers: 5'-TGG GAT TAC ACG TGT GAA CCA ACC-3' and 5'-GCT CTA CCC TCT CCT CTA CCG TCC-3' for HPRT and 5'-CAT GTC ACC ACT GGA CTC TGA AC-3' and 5'-CCT GGA GTA GGA ACA AA ATT GCT-3' for POLB. Preliminary assays were carried out to ensure the linearity of PCR amplification with respect to the number of cycles and DNA concentration. The final PCR reaction condition was standardized at 94°C-30 sec⁻¹ cycle; 94°C-30 sec, 58°C 30 sec, 65°C 10 min for 25 cycles; 65°C 10 min⁻¹ cycle and 15 ng of DNA template was used for each reaction. Since amplification of a small region would be independent of DNA damage, a small DNA fragment

was also amplified for normalization of long amplicons using the following primers: 5'-TGC TCG AGATGT GAT GAA GG-3' and 5'-CTG CAT TGT TTT GCC AGT GT-3' for HPRT; 5'-AGT GGG CTG GAT GTA ACCTG-3' and 5'-CCA GTA GAT GTG CTG CCA GA-3' for POLB. The amplified products were then visualized on gels and quantitated with ImageJ automated digitizing system on the basis of three replicate gels in each case.

Conclusions

Genotoxic-risks have been identified during the treatment systemic fungal infection with amphotericin B or anidulafungin. AMP-B reflects higher affinity to damage DNA than anidulafungin. Simultaneously, increase in the level of the DNA repair proteins, the higher level of DNA SB accumulation in case of treatment with amphotericin B could possess serious threat to normal cell survival and thus, anidulafungin may be a preferred choice for antifungal treatment. DNA repair or antioxidant therapy is necessary during antifungal drugs administration.

Acknowledgement

Authors are gratefully acknowledging IIT-Kharagpur for providing the instrumental facility. The work was also supported by the grant (NIH NS07397604) to T.K.H.

Notes and references

- 1 J.A. Vazquez, and J.D. Sobel, Anidulafungin: A novel echinocandin, *Clin Infect Dis*, 2006; **11**, 215-222.
- 2 M.H. Nguyen, J.E. Peacock, A.J. Morris, D.C. Tanner, M.L. Nguyen and D.R. Snyderman, et al., The changing face of candidemia: emergence of non-*Candida albicans* species and antifungal resistance, *Am J Med*, 1996, **100**, 617-623.
- 3 T. Gumbo, C.M. Isada, C.M. Hall, M.T. Karafa, and S.M. Gordon, *Candida glabrata* Fungemia-Clinical features of 139 patients, *Medicine*, 1999, **78**, 220-227.
- 4 B.D. Alexander, W.A. Schell, J.L. Miller, G.D. Long, and J.R. Perfect, *Candida glabrata* fungemia in transplant patients receiving voriconazole after fluconazole, *Transplantation*, 2005, **80**, 868-871.
- 5 T. Gumbo, G.L. Drusano, W. Liu, L. Ma, M.R. Deziel, and M.F. Drusano, et al., Anidulafungin pharmacokinetics and microbial response in neutropenic mice with disseminated candidiasis, *Antimicrob Agents Chemother*, 2006, **50**, 3695-3700.
- 6 J. Chaires. Energetics of drug-DNA interactions, *Biopolym*, 1997, **44**, 201-215
- 7 J.B. Chaires, N. Dattagupta and D.M. Crothers, Studies on interaction of anthracycline antibiotics and deoxyribonucleic acid: equilibrium binding studies on the interaction of daunomycin with deoxyribonucleic acid, *Biochem*. 1982, **21**, 3933-3940.
- 8 J.D. McGhee, P.H. von Hippel, Theoretical aspects of DNA-protein interactions: Co-operative and non-co-operative binding of large ligands to a one-dimensional homogeneous lattice, *J Mol Biol*. 1974, **86**, 469-489.
- 9 A.W. Schüttelkopf and D.M.F. Van-Aalten. PRODRG: a tool for high-throughput crystallography of protein-ligand complexes, *Acta Crystallogr D*, 2004, **60**, 1355-1363.
- 10 H. Yuan, J. Quintana and R.E. Dickerson. Alternative structures for alternating poly(dA-dT) tracts: the structure of the B-DNA decamer C-G-A-T-A-T-A-T-C-G, *Biochem*, 1992, **31**, 8009-8021.
- 11 V. Tereshko, C.J. Wilds, G. Minasov, T.P. Prakash, M.A. Maier and A. Howard, et al., Detection of alkali metal ions in DNA crystals using state-of-the-art X-ray diffraction experiments, *Nucleic Acids Res*, 2001, **9**, 1208-1215.
- 12 D.S. Goodsell, K. Grzeskowiak and R.E. Dickerson. Crystal structure of C-T-C-T-C-G-A-G-A-G. Implications for the structure of the Holliday junction, *Biochem*. 1995, **34**, 1022-1029.
- 13 O. Trott and A.J. Olson, AutoDock Vina: improving the speed and accuracy of docking with a new scoring function, efficient optimization, and multithreading, *J Comput Chem*. 2010, **1**, 455-461.
- 14 G.M. Morris, R. Huey, W. Lindstrom, M.F. Sanner, R.K. Belew, D.S. Goodsell and A.J. Olson. AutoDock4 and AutoDockTools4: Automated docking with selective receptor flexibility, *J Comput Chem*, 2009, **30**, 278527-91.
- 15 S.M. Mandal, L. Migliolo, S. Das, M. Mandal, O.L. Franco and T.K. Hazra, Identification and characterization of a bactericidal and proapoptotic peptide from *Cycas revoluta* seeds with DNA binding properties, *J Cell Biochem*. 2012, **113**, 184-93.
- 16 J.H. Santos, J.N. Meyer, B.S. Mandavilli and B.V. Houten. Quantitative PCR-based measurement of nuclear and mitochondrial DNA damage and repair in mammalian cells, *Methods Mol Biol*, 2006, **314**, 183-199.
- 17 S. Dey, A.K. Maiti, M.L. Hegde, P.M. Hegde and I. Boldogh et al., Increased risk of lung cancer associated with a functionally impaired polymorphic variant of the human DNA glycosylase NEIL2, *DNA Repair*, 2012, **11**, 570-578.
- 18 M. Hossain and G.S. Kumar. DNA intercalation of methylene blue and quinacrine: New insights into base and sequence specificity from structural and thermodynamic studies with polynucleotides, *Mol. Biosystems*, 2009, **5**, 1311-1322.

- 19 A. Jilani, D. Ramotar, C. Slack, C. Ong, X.M. Yang and S.W. Scherer, et al. Molecular cloning of the human gene, PNKP, encoding a polynucleotide kinase 3'-phosphatase and evidence for its role in repair of DNA strand breaks caused by oxidative damage, *J Biol Chem*, 1999, **274**, 24176-24186.
- 20 D. Banerjee, S.M. Mandal, A. Das, M.L. Hegde, S. Das and K.K. Bhakat, et al., Preferential repair of oxidized base damage in the transcribed genes of Mammalian cells, *J Biol Chem*. 2011, **286**, 6006-6016.

Conflict of interest: None

Abbreviations: Amphotericin B, AMP-B; Anidulafungin, ANIDULA; Ultraviolet-visible spectroscopy, UV-Vis; isothermal titration calorimetry, ITC; circular dichroism, CD; The long amplicon quantitative PCR for DNA damage, LA-QPCR; Chinese Hamster Ovary, CHO; Food and Drug Administration, FDA; 3-(4,5-dimethylthiazol-2-yl)-5-(3-carboxymethoxyphenyl)-2-(4-sulfophenyl)-tetrazolium, MTT; Human Embryonic kidney, HEK-293.

Figure legends:

Fig. 1. Representative chemical structure of amphotericin B and anidulafungin.

Fig. 2. Absorption spectral changes of (A) anidulafungin- (5 μ M) treated with 0, 5, 10, 15, 20 and 25 μ M (curves 1–6) of DS-DNA and (B) amphotericin B (5 μ M) treated with 0, 5, 10, 15, 20, 25 and 30 μ M (curves 1–7) DS-DNA. Inset: shows a fitting of the absorbance data used to obtain the binding constants.

Fig. 3. ITC profiles for the binding of (A) anidulafungin to AG-DNA and (B) Amphotericin B to GC DNA. Top panels present raw results for the sequential injection of (A) AG-DNA and (B) GC DNA in citrate-phosphate buffer, pH 7.01 at 25 $^{\circ}$ C. The bottom panels show the integrated heat results after correction of heat of dilution against the mole ratio. The data points were fitted to one site model and the solid lines represent the best-fit data.

Fig. 4. Intrinsic circular dichroic (far UV) spectral changes of (A) amphotericin B -DS DNA (30 μ M) and (B) anidulafungin-DS DNA (30 μ M). In panel (A) curves 1 to 4 denote 0, 30, 45, and 60 μ M of amphotericin B, panel (B) curves 1 to 4 denote 0, 30, 45, and 60 μ M of anidulafungin.

Fig. 5. Molecular docking results. (A) The average binding energy of 50 samples of molecular docking of amphotericin B (blue) and anidulafungin (orange) against the four SS DNA. Overall, amphotericin B binds with a lower energy, resulting in more affinity than anidulafungin. (B and C) Complexes of amphotericin B (white backbone) and SS DNA (blue backbone) of AG and AT, respectively. The complexes are kept through a number of hydrogen bonds (yellow dotted lines). The sequence of SS DNA is also indicated. The two complexes showed virtually the same energy retrieved from ITC experiments, -6.7 and -6.3 Kcal.mol⁻¹ for amphotericin B -AG and amphotericin B -AT, respectively.

Fig. 6. Genotoxic effect of the antifungal drugs in terms of expression level of DNA repair proteins. Panel A: anidulafungin treatment. Panel B: amphotericin B treatment. Con: Control (mock or without treatment) and rest of the lanes indicate treatment with antifungal agent with increasing concentration (in the unit of μ g/ml). The whole cell extract, after treatment with the different concentration of the antifungal agents for 24 hrs, were probed with various DNA repair proteins (indicated at the left) to estimate their expression profiles. Lamin B was used as loading control to

check for equal loading in each case. Panels C and D show the histograms representing fold changes of expression level of various DNA repair proteins (normalized with loading control) after treatment with different doses of anidulafungin and amphotericin B, respectively and quantified by ImageJ.

Fig. 7. Analysis of genotoxic effect in terms of DNA strand break accumulation. Panel A: anidulafungin treatment. Panel B: amphotericin B treatment. Con: Control (mock or without treatment) and rest of the lanes indicate treatment with antifungal agent with increasing concentration (in the unit of μ g/ml). The genomic DNA was extracted after treatment with the different concentration of the antifungal agents for 24 hrs, and subjected to LA-PCR with oligos specific for HPRT. Short intron specific fragment of the gene was used as control for normalization. Panels C and D show histograms representing the DNA damage quantitation for different treatments (n=3). Error bars indicate standard error of means.

TABLE 1 : Isothermal calorimetric data for the binding of anidulafungin (anidula) and Amphotericin B (AMP-B) to polynucleotides at 25°C

Polynucleotides	Drug	N	$K \times 10^{-5}$ (M^{-1})	ΔG (kcal /mol)	ΔH (kcal /mol)	$T\Delta S$ (kcal /mol)
DS						
	Anidula	5.94±0.32	0.56±0.0134	-6.45±0.16	-68.46±0.16	-62.01
	Amp-B	4.30±0.101	1.05±0.123	-6.85±0.13	-13.67±0.13	-6.82
AG						
	Anidula	3.55±0.0922	1.94±0.36	-7.21±0.39	-40.61±0.39	-33.40
	Amp-B	5.40±0.160	0.847±0.016	-6.72±0.11	-2.69±0.114	4.03
AT						
	Anidula	nd	nd	nd	nd	nd
	Amp-B	2.17±0.063	0.53±0.042	-6.45±0.10	4.57±0.10	11.02
GC						
	Anidula	nd	nd	nd	nd	nd
	Amp-B	4.69±0.027	2.75±0.160	-7.42±0.57	-72.44±0.57	-65.02
TC						
	Anidula	4.18±0.350	0.793±0.034	-6.68±0.16	9.11±0.162	15.79
	Amp-B	2.72±0.0389	1.90±0.16	-7.21±0.88	-45.79±0.88	-38.76

All the data in this table are derived from ITC experiment are average of four determinations. K and ΔH values were determined from ITC profiles fitting to Origin 7 software as described in the text. The values of ΔG and $T\Delta S$ were determined using the equations $\Delta G = -RT \ln K$, and $T\Delta S = \Delta H - \Delta G$. All the ITC profiles were fit to a model of single binding sites.

Figure 1.

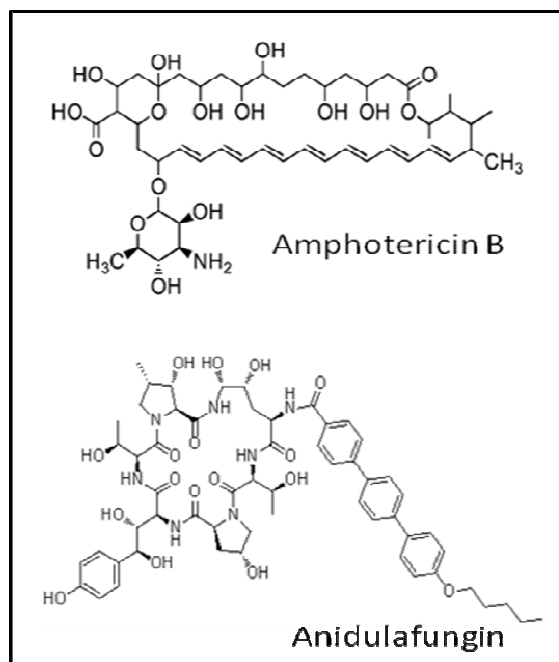


Figure 2.

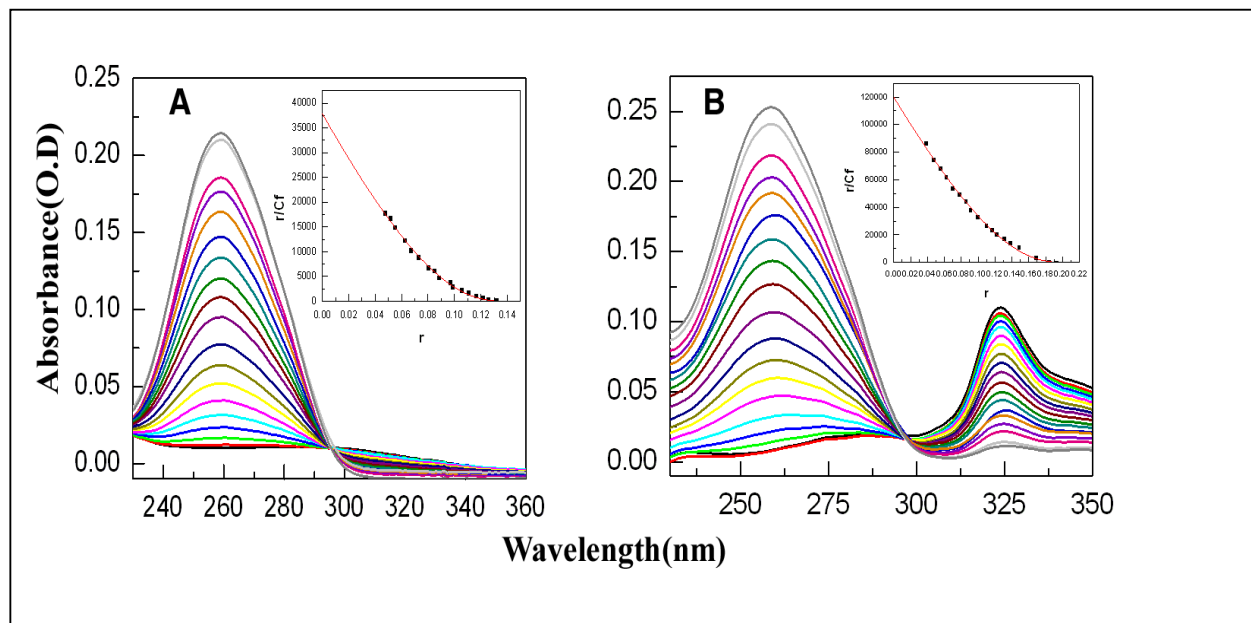


Figure 3.

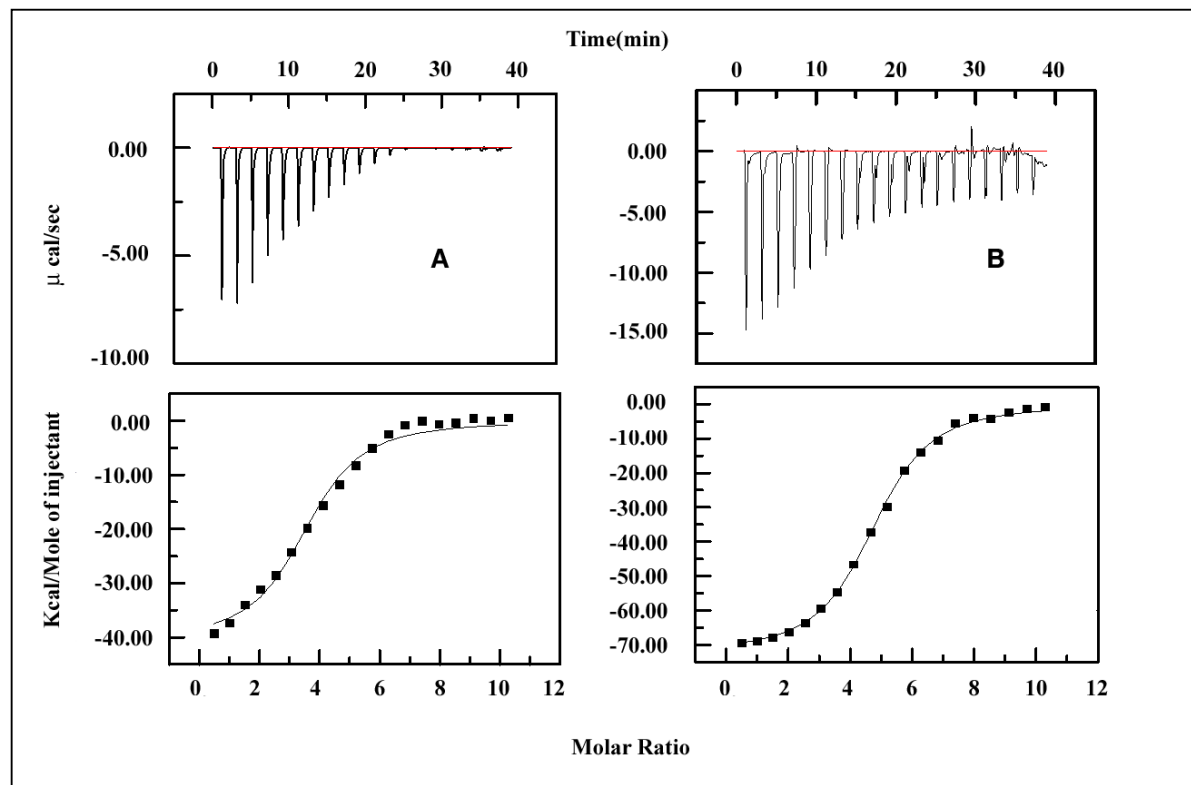


Figure 4.

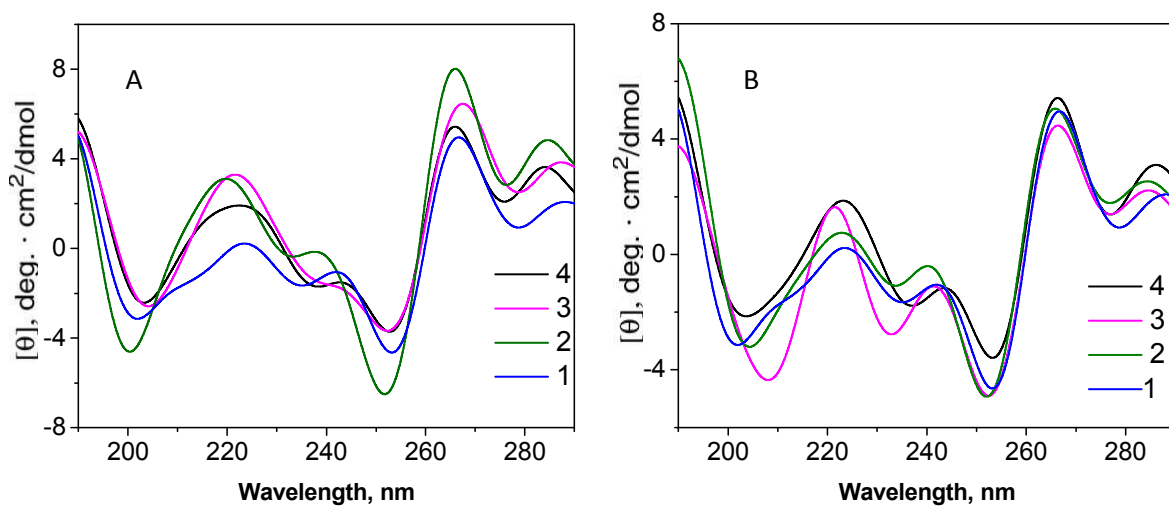


Figure 5.

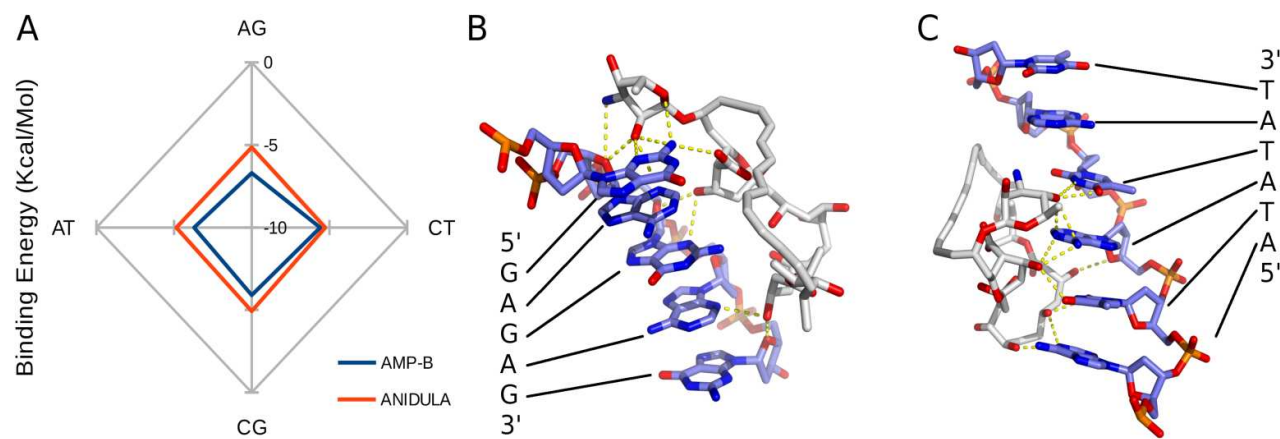


Figure 6.

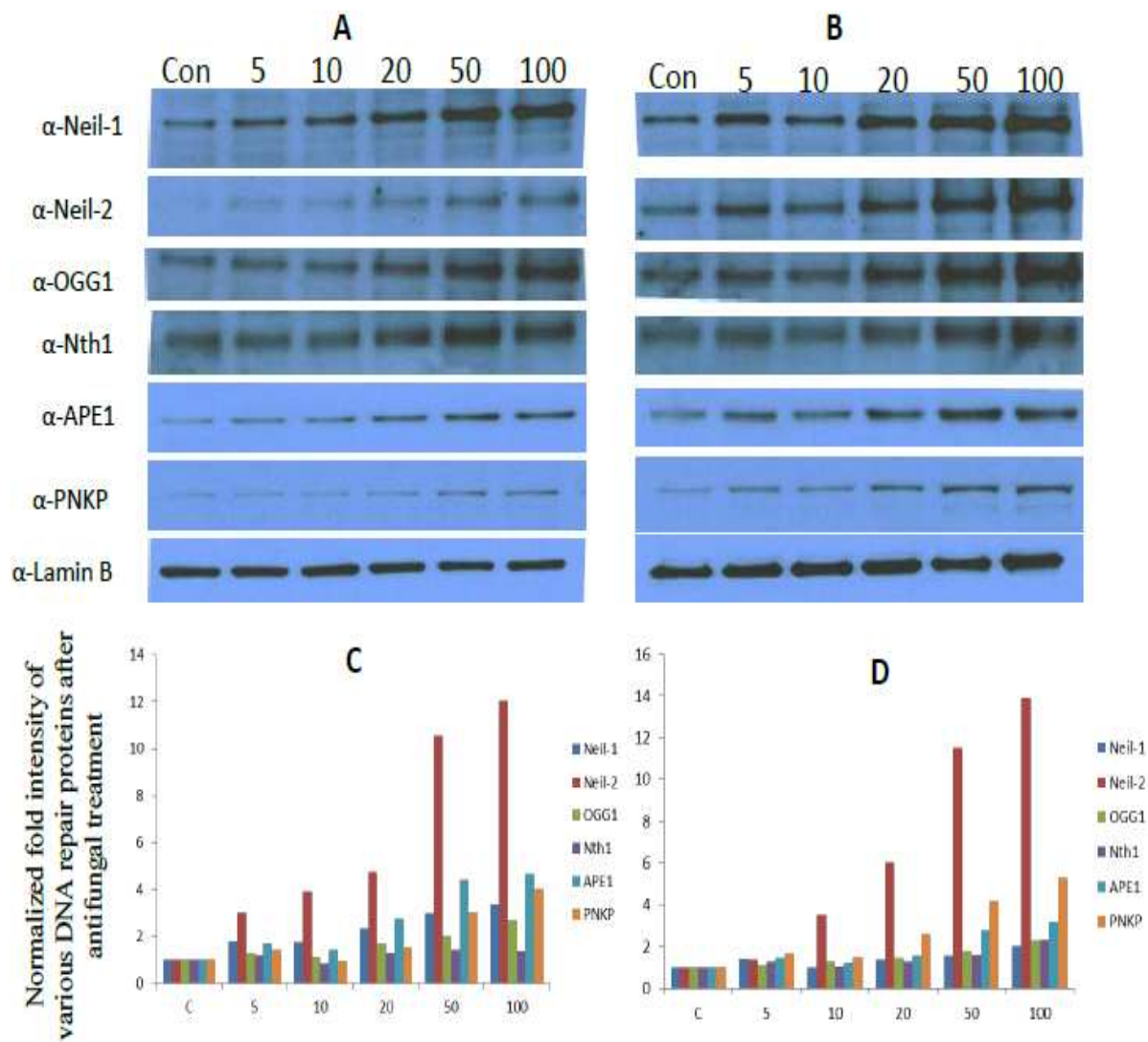


Figure 7.

